Supplementary Information (SI) for Physical Chemistry Chemical Physics.
This journal is © the Owner Societies 2026

2D correlation spectroscopy for EC-SERS of organic molecules at free-floating AuNP films

Madjid Tarabet,[1] Yinxi Zou,[1] Dyia Syaleyana Md Shukri,[1,2,3] Noorfatimah Yahaya,[3] Manuel Dossot,[1] Grégoire Herzog[1*]

[1]: Université de Lorraine, CNRS, LCPME, F-54000 Nancy, France.

[2]: Department of Toxicology, Advanced Medical and Dental Institute (AMDI), Universiti Sains Malaysia, 13200 Bertam Kepala Batas, Pulau Pinang, Malaysia.

[3]: Faculty of Applied Sciences, Universiti Teknologi MARA (UiTM) Perlis, Kampus Arau, 02600 Arau, Perlis, Malaysia.

Corresponding authors: manuel.dossot@univ-lorraine.fr; gregoire.herzog@cnrs.fr

Table of contents

S.I. Electrochemical and spectro-electrochemical set-ups

S.I.1. 4-electrode cell

Liquid-liquid electrochemistry experiments were done at custom-made glass cell (Figure S1). The surface area of the interface was 1.13 cm^2. Two platinum counter-electrodes were used, immersed in the aqueous phase and organic phase, respectively. Additionally, two silver wires coated with a layer of silver chloride served as reference electrodes (Ag/AgCl) immersed in the aqueous phase and organic reference phase of 100 mM NaCl and 2.5 mM bis(triphenylphosphoranylidene)ammonium chloride (BACl). The composition of the organic phase remained constant throughout all electrochemical experiments, with 2.5 mM of bis(triphenylphosphoranylidene)ammonium tetrakis(pentafluorophenyl)borate (BATB) dissolved in TFT.

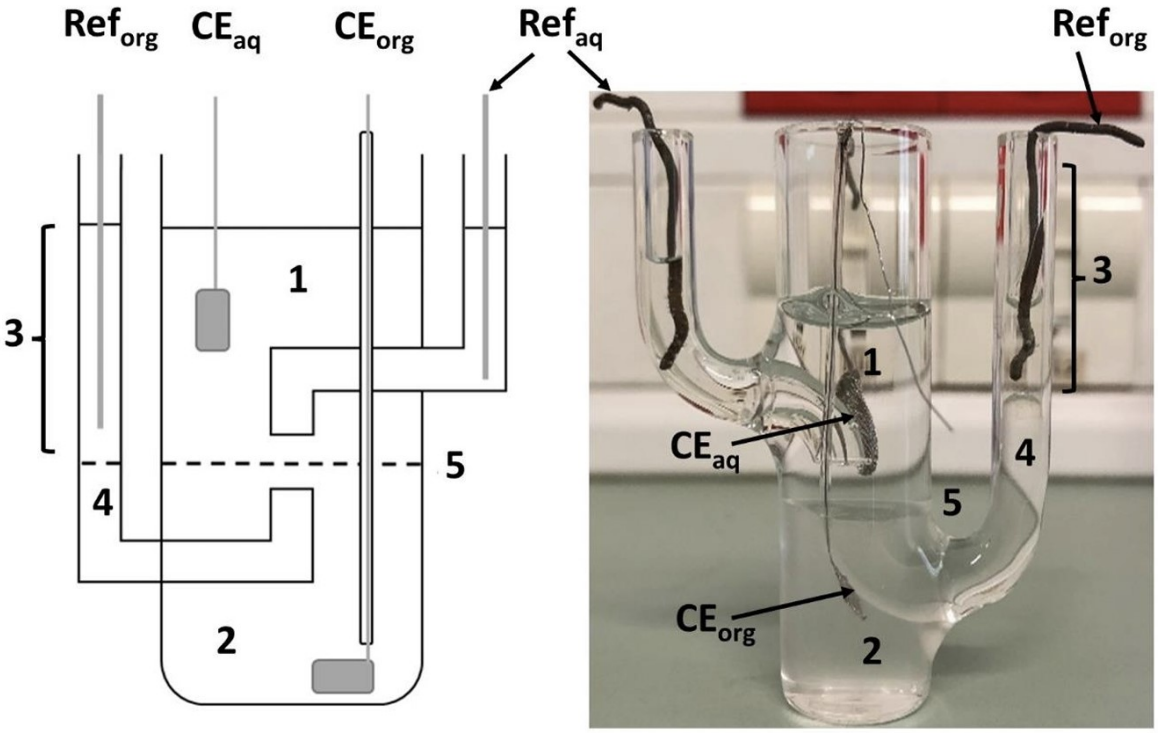

Figure S1: Schematic representation (left) and photograph (right) of a custom made 4-electrode electrochemical cell. **CE_{org}** *and* **CE_{aq}** *correspond to organic and aqueous counter-electrodes respectively, and* **RE_{org}** *and* **RE_{aq}** *represent the organic and aqueous reference electrodes. 1 – aqueous phase (aq); 2 – organic phase (org); 3 – aqueous solution for organic reference electrode; 4 – liquid-liquid interface formed between the organic phase and the aqueous solution for organic reference electrode; 5 – interface between the two electrolyte solutions (ITIES). The volume of both phases is 2.9 mL.*

S.I.2 EC-SERS experimental set-up

We also designed a custom electrochemical cell for *in-situ* and *operando* EC-SERS measurements, allowing the laser to be directly focused on the gold nanoparticle (AuNP) film formed at the ITIES. This electrochemical cell, with a diameter of 43.7 mm and phase volumes reaching up to 17 mL, is specifically adapted for a water immersion objective (focusing on the aqueous phase), the counter electrodes in both the aqueous and organic phases are made of 316L stainless steel (Figure S2).

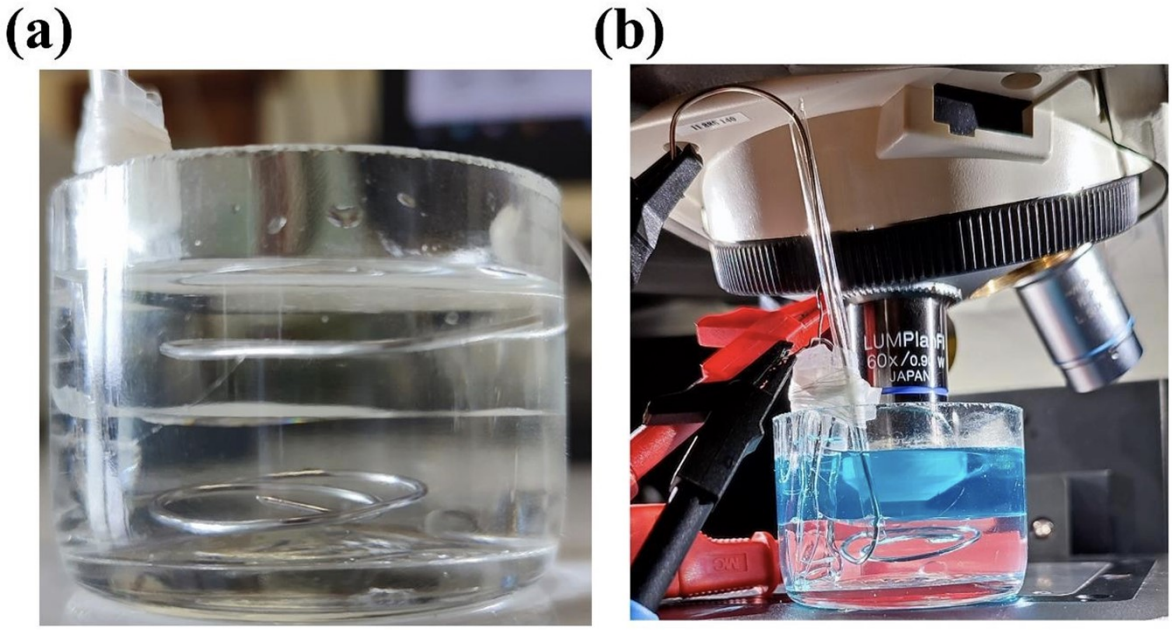

Figure S2: (A) Photographs of the electrochemical cell used for Raman spectroelectrochemical experiments. (B) 4-electrode spectroelectrochemical cell with an immersion objective used for the SERS experiments on electrogenerated AuNP films. The aqueous solution contained methylene blue.

S.I.3 TIR spectro-electrochemical set-up

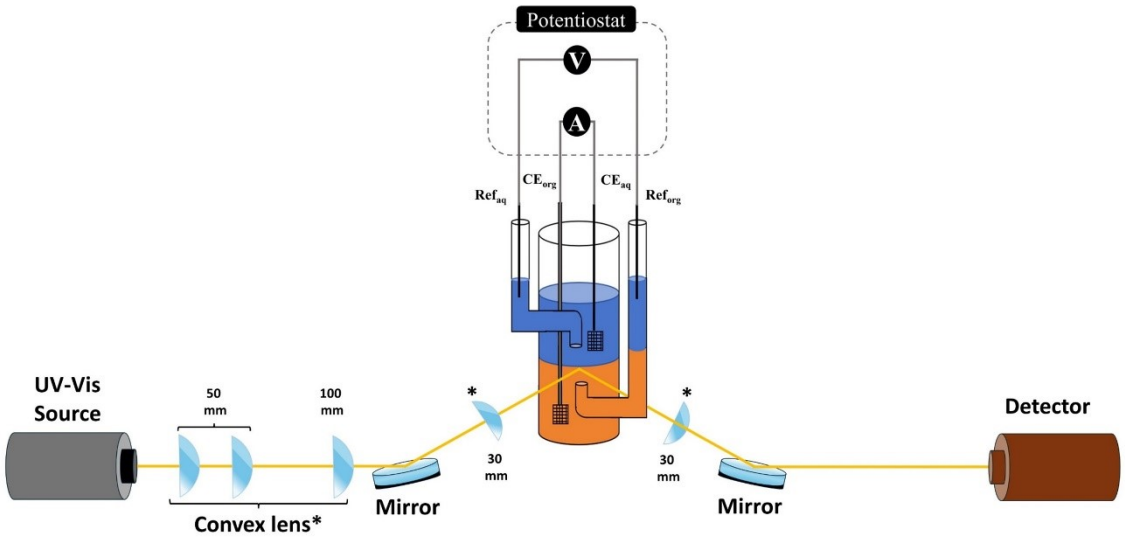

Figure S3: Schematic representation of the set-up used for the electrochemical experiments coupled to Total Internal Reflectance (TIR) absorption spectroscopy measurements.

S.II. TIR spectro-electrochemical measurements

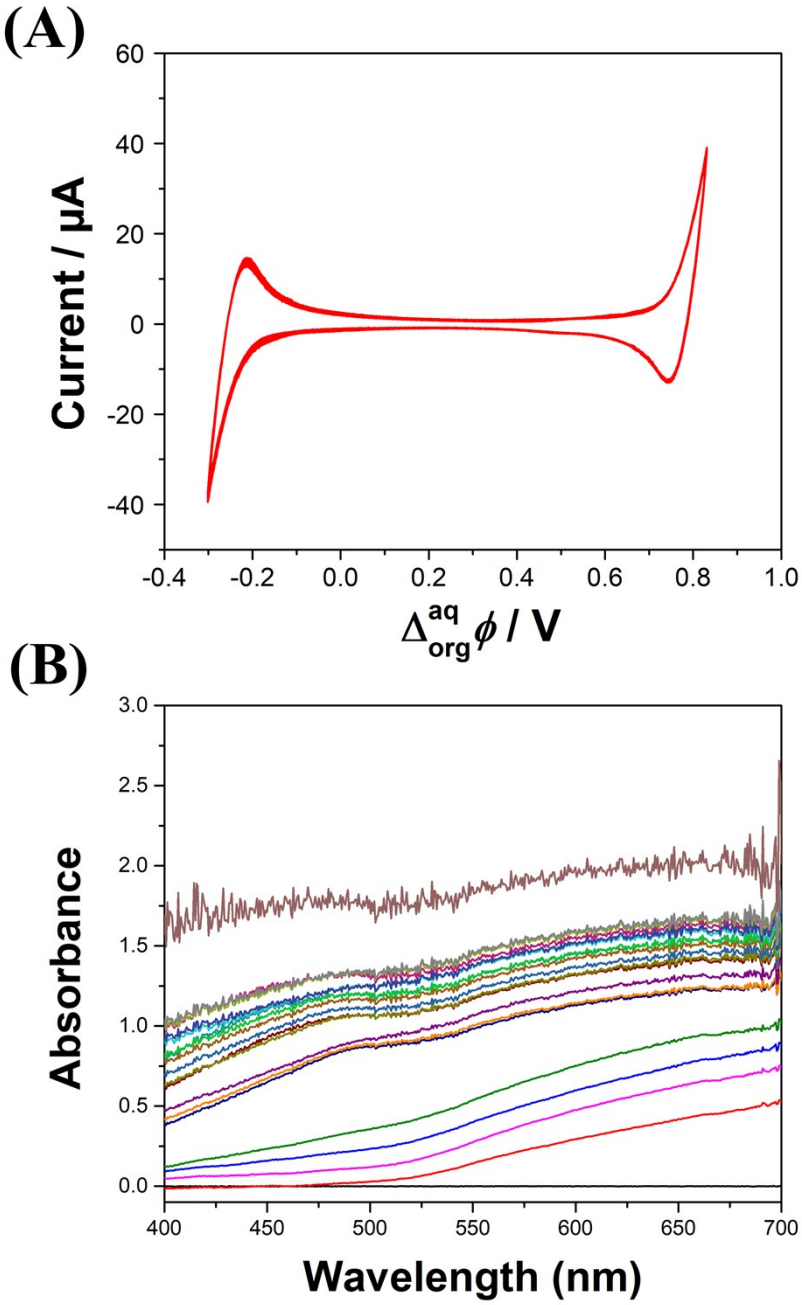

Figure S4: (A) CV of the electrogeneration of AuNP films with $C_0/3$, $\nu = 20\ mV\ s^{-1}$, 90 cycles. (B) Evolution of absorbance with the number of cycles during the Au NP film electrogeneration shown in (A). For simplicity, only spectra after cycles 0, 3, 5, 7, 10,15, 20, 30, 40, 50, 60, 70, 80, and 90 are shown. Black curve represents the absorbance before the electrogeneration of the AuNP film.

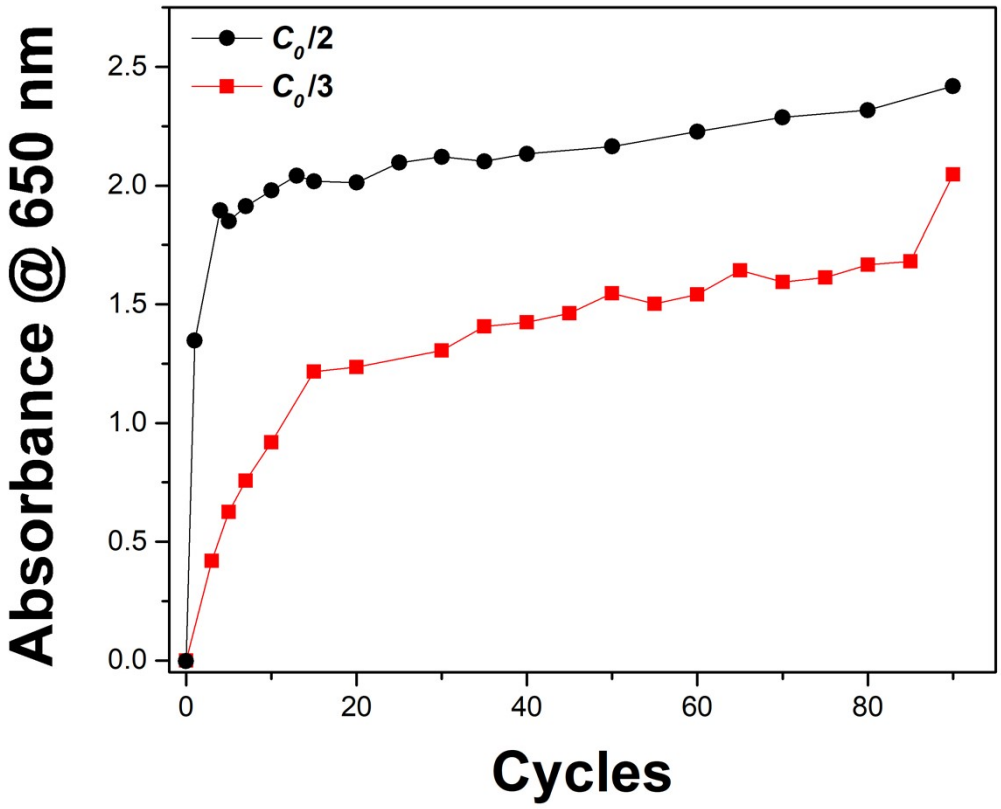

Figure S5: Evolution of the Absorbance @650 nm as a function of the number of cycles. TIR spectra were measured at open-circuit potential between two cycles.

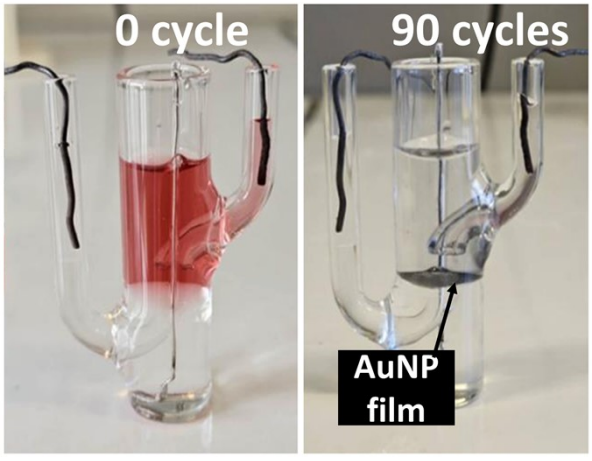

Figure S6: Photographs of the electrochemical cell before and after 90 cycles. Initial concentration of nanoparticles was C_0 / 3. For clarity, the counter electrode of the aqueous phase is not present on the pictures.

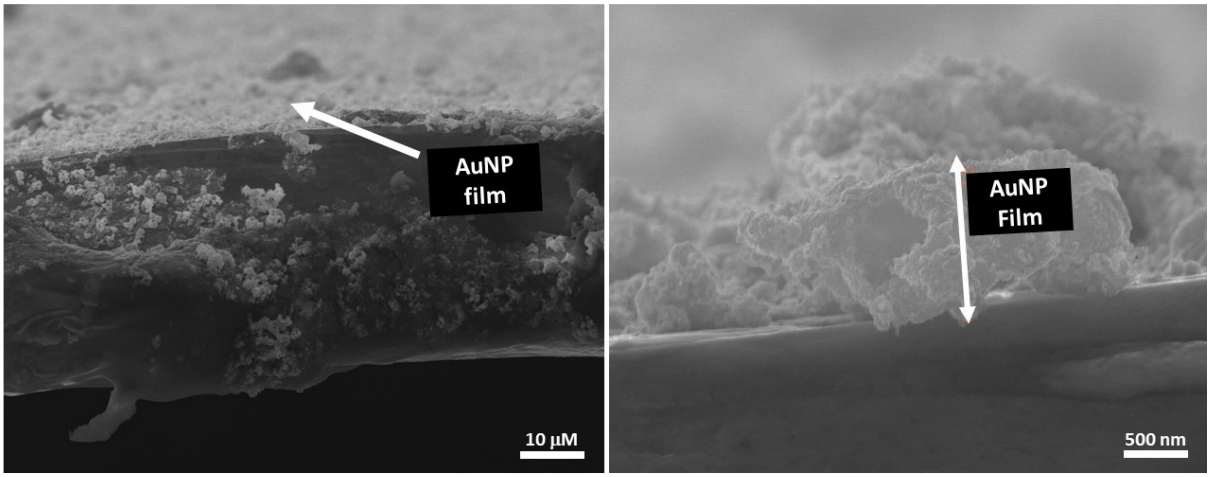

Figure S7: SEM micrographs of the AuNP films formed at the ITIES from a $C_0/2$ colloidal suspension

S.III. EC-SERS of AuNP films

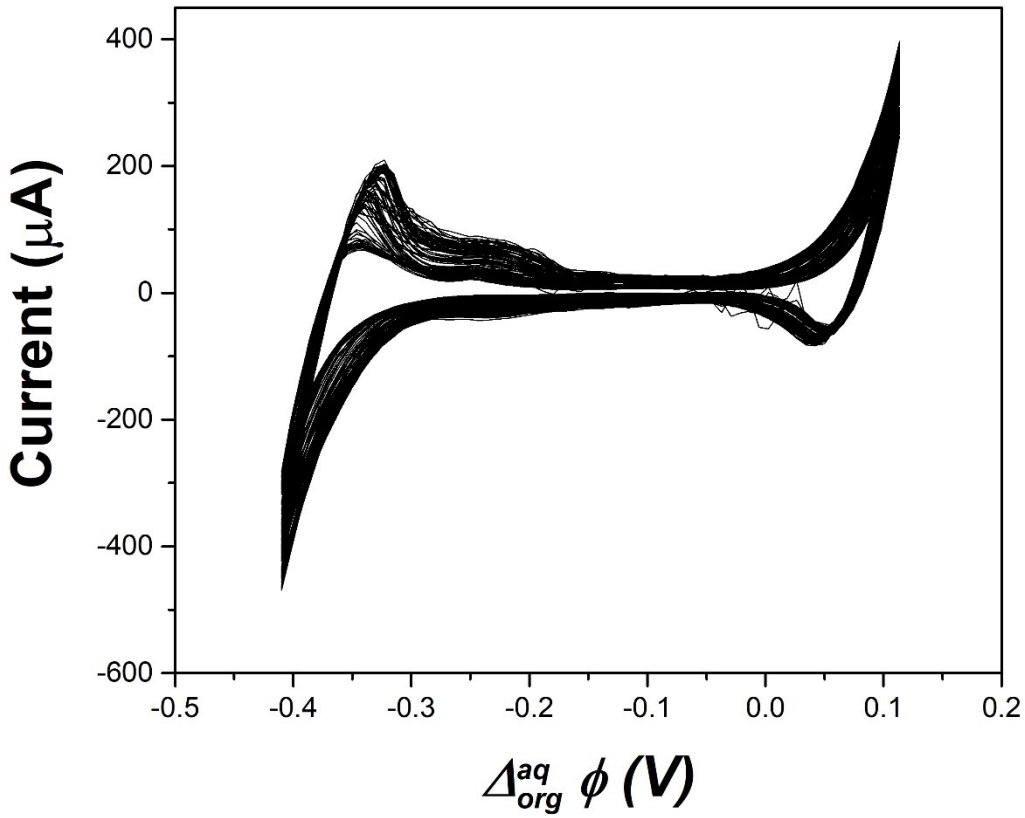

Figure S8: Voltammogram over 90 cycles showing the formation of a NP film at a liquid-liquid interface. The organic phase contains 2.5 mM BATB, and the aqueous phase contains gold nanoparticles at a concentration of $C_0/2$. The scan rate is 20 mV s^{-1}.

In all three experimental conditions, the spectra were dominated by a peak at 1003 cm^{-1}, which corresponded to the symmetric elongation of the C-C bonds of the aromatic rings, common to both the solvent molecules and the organic cation BA^+. Other peaks, characteristic of BA^+ cations and solvent molecules were recorded at 770, 1027, and 1324 cm^{-1}. Once AuNPs were present in the aqueous phase but before any potential cycling was applied, the same features were observed with the appearance of two small peaks at 1161 and 1188 cm^{-1}. They were characteristics of the organic cation BA^+ as they correspond to out-of-plane deformation of C-H bonds of the benzoic ring. Their observation was made possible by the presence of negatively covered Au NPs, which may suggest the spontaneous adsorption of a very thin AuNP film, not visible by the naked eye. After the 90 cycles, the intensity of all peaks increased by a factor 2, confirming that the presence of the film allowed the SERS effect of the solvent molecules and of the background electrolyte as was reported by Dryfe and co-workers [1].

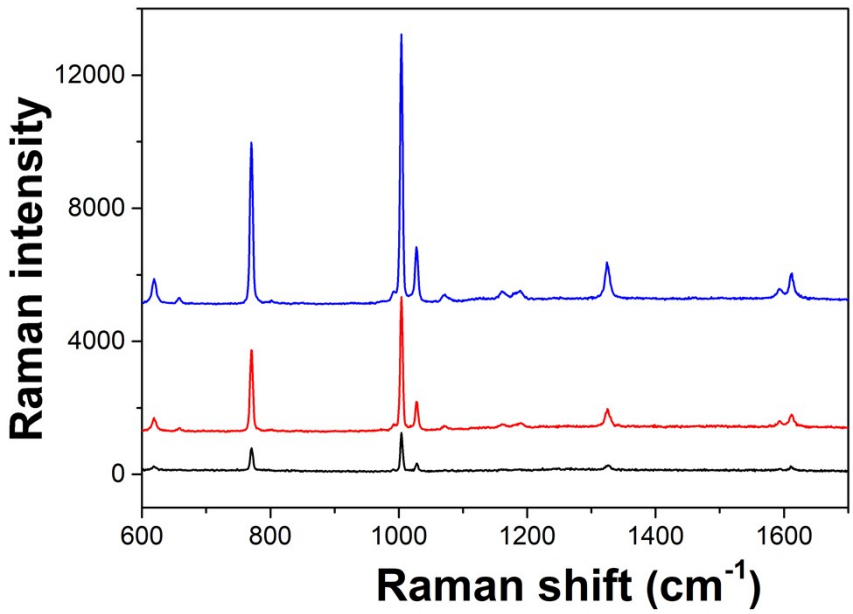

Figure S9: Raman spectra of a water | 2.5 mM BATB in TFT interface (black curve); of a AuNP colloidal suspension | 2.5 mM BATB in TFT interface before electrochemical formation of the film (red curve) and a AuNP film || 2.5 mM BATB in TFT interface (blue curve). λ = 785 nm (10 % laser power).

S.IV. EC-SERS of Nor^+

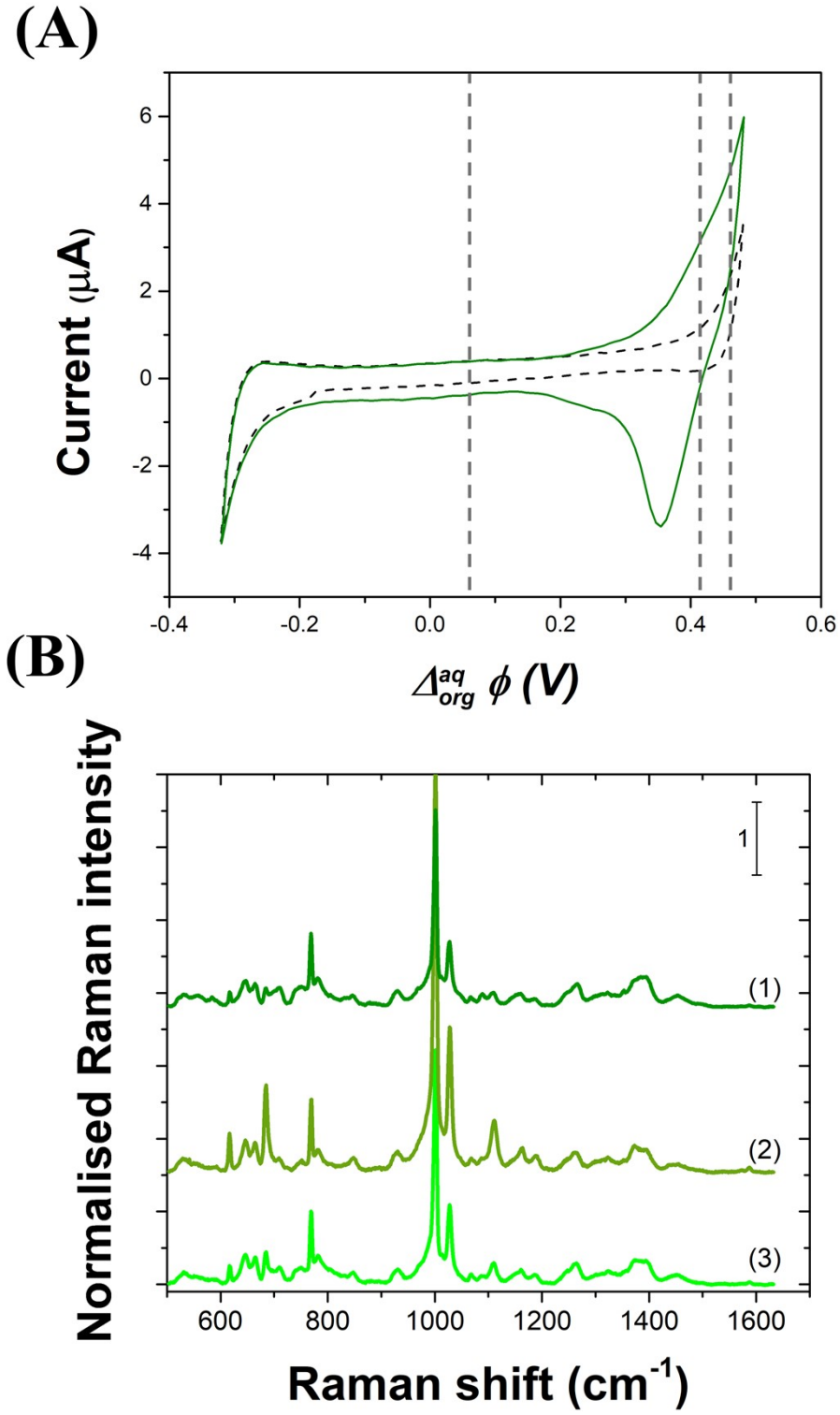

Figure S10: (A) CV of 10 μM Nor^+ at the ITIES. Blank CV is shown as black dashed lines. ν = 20 mV s^{-1}. CVs were recorded in the absence of AuNP film. (B) Average SERS spectra (N = 100) measured at

electrogenerated AuNP films for different $\Delta_{org}^{aq}\phi$ *values: (1)* $\Delta_{org}^{aq}\phi = +0.45\,V$*, (2)* $\Delta_{org}^{aq}\phi = +0.41\,V$*, and (3)* $\Delta_{org}^{aq}\phi = +0.05\,V$*. These potential values are indicated as dashed lines on (A).*

S.V. 2D correlation of MB^+ EC-SERS

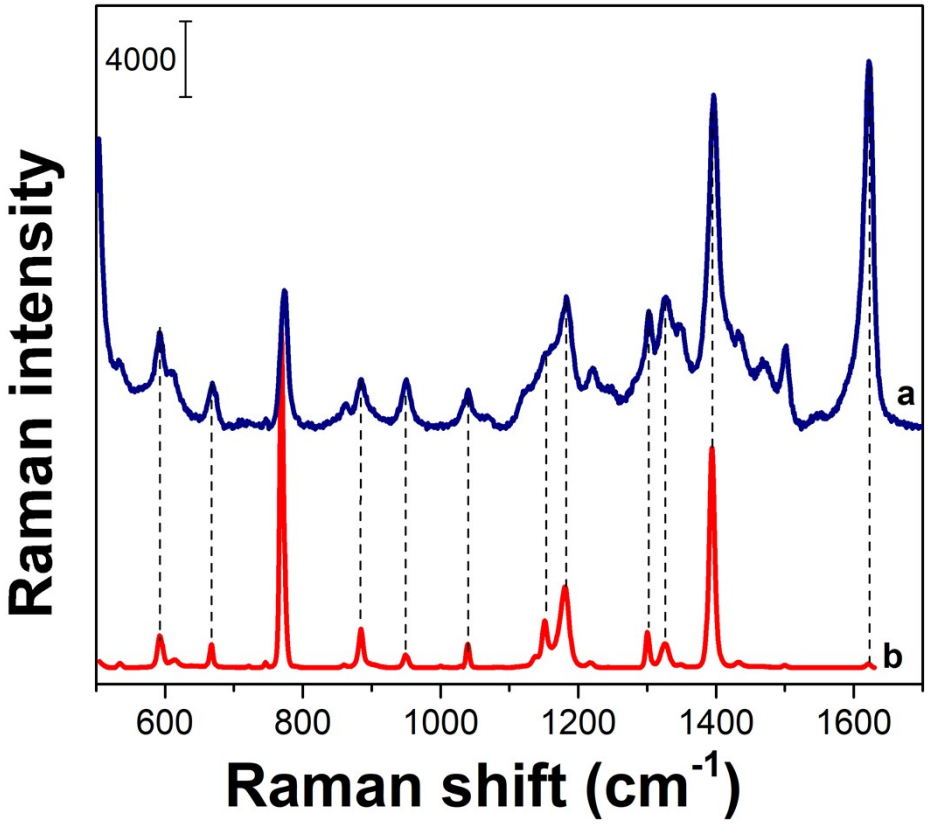

Figure S11: Comparison of (a)conventional SERS spectrum of the MB^+ *cations obtained in a suspension of gold NP aggregated with NaCl with (b) the autocorrelation spectrum (represented by the dashed line shown in Figure 4A).*

S.VI. DFT calculation of the Raman peaks for MB^+, Nor^+ and BA^+

The geometry of the MB^+ cation was optimized using the density functional theory (DFT) using Gaussian 2016 software. Becke three hybrid exchange (B3) and Lee-Yang-Parr (LYP) functional, and 6311G++(2d,2p) basis set were used for geometry optimization and Raman and infrared frequencies calculation. Water solvent was simulated using a polarized continuum model (IEFPCM). Table S1 only reports the Raman frequencies, unscaled and scaled by 0.98 since it is known that DFT calculations with these functionals and basis set generally overestimate the vibrational frequencies. The three Raman peaks discussed in the article are highlighted in yellow in Table S1.

Table S1: Raman vibrational frequencies for methylene blue cation calculated by DFT B3LYP 6311G++(2d,2p) with IEFPCM model to simulate water solvent:

Mode	Calculated Raman shift cm^{-1}	Measured Raman shift cm^{-1}	Assignment[a]
31	591	593	In-plane bending of (C—N—C) attached to the methyl group
37	759	770	stretching of (C—N) attached to the methyl group; in-plane bending of the (C—N—C) ring
44	878	884	in-plane bending of the (C—C—C) ring
60	1176	1180	CH_3 rocking; in-plane bending of CH
65	1302	1302	in-plane bending of CH; stretching of (C—N) ring
69	1389	1392	stretching of (C—N) ring; in-plane bending of CH
90	1627	1624	Stretching of the (C—C) and (C—N) rings

[a]: assigned in agreement with ref [2]

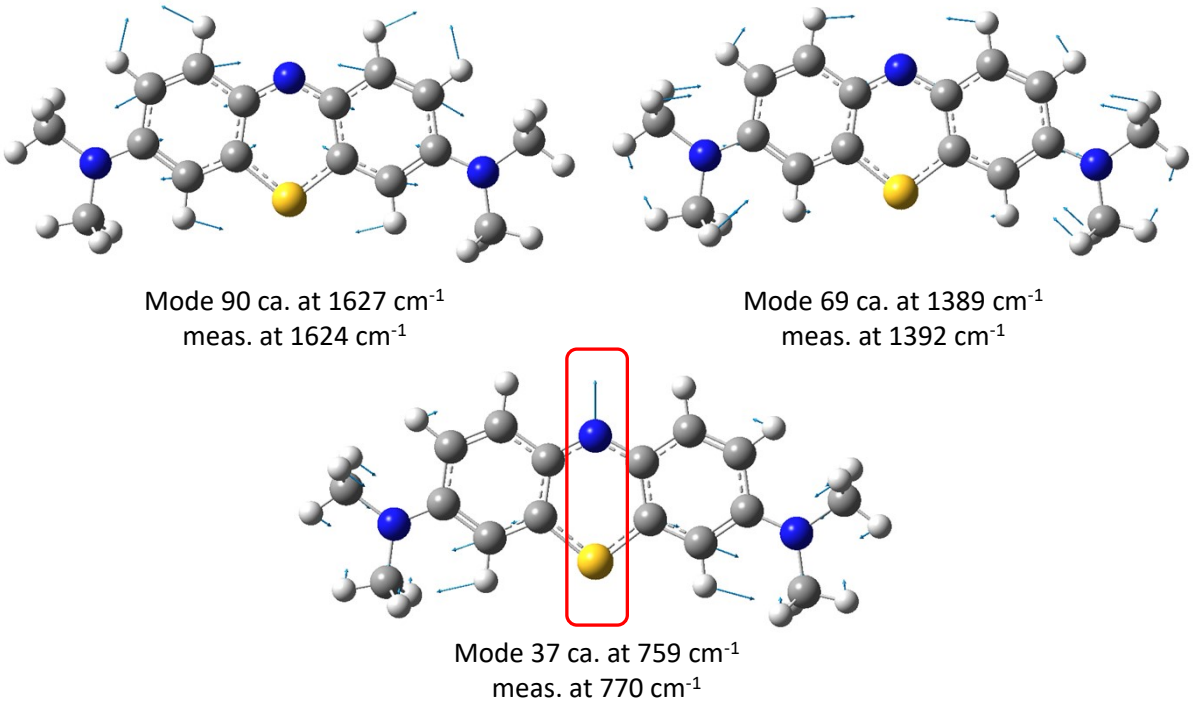

Figure S12: Displacement vectors calculated by DFT for the three Raman peaks of methylene blue cation discussed in the text of the article.

Table S2: Raman vibrational frequencies for BA^+ calculated by DFT B3LYP 6311G++(2d,2p) with IEFPCM model to simulate water solvent:

Mode	Calculated Raman shift cm^{-1}	Measured Raman shift cm^{-1}	Assignment
1	619	617	Symmetric stretching of aromatic C-C
2	654	662	Stretching of N=P bonds
4	995	1001	Stretching of aromatic C-C
5	1023	1027	Stretching of aromatic C-C
6	1091	1100	Stretching of P -$C_{aromatic}$ bonds

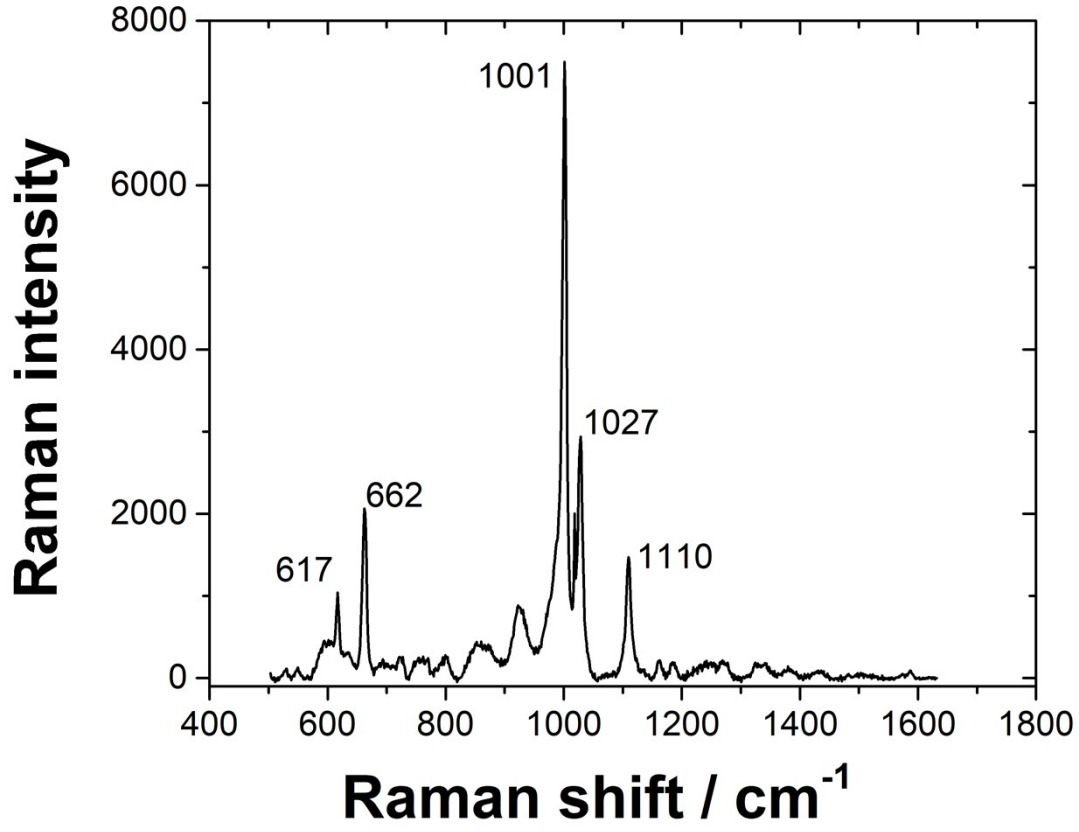

Figure S13: Raman spectra of BACl powder as a control. The numbers indicate the Raman shift of the most prominent BA^+ peaks.

Table S3: Raman vibrational frequencies for Nor$^+$ calculated by DFT B3LYP 6311G++(2d,2p) with IEFPCM model to simulate water solvent:

Mode number	Calculated Raman shift cm^{-1}	Measured Raman shift cm^{-1}	Assignement
1	1260	1266	CH_2 rocking and twisting, NH_2 rocking, C6-C1-H7 scissoring, phenyl ring deformation
2	1295	--	CH_2 wagging and twisting, NH_2 twisting, phenyl ring deformation, C26-C27-H28 scissoring
3	1337	--	CH2 wagging and twisting, phenyl ring deformation, C26-C27-H28 scissoring **but NH_2 is not moving**
4	1368	1353	CH_2 and NH_2 twisting+C6-C1-H7 scissoring, phenyl ring deformation, ethyl CH_3 umbrella bending, C26-C27-H28 scissoring
5	1378	1373	CH_2 and NH_2 twisting, ethyl CH_2 wagging, ethyl CH_3 umbrella bending, C26-C27-H28 scissoring
6	1412	1394	NH_2 and CH_2 wagging, ethyl CH_2 wagging, ethyl CH_3 umbrella bending, phenyl ring deformation

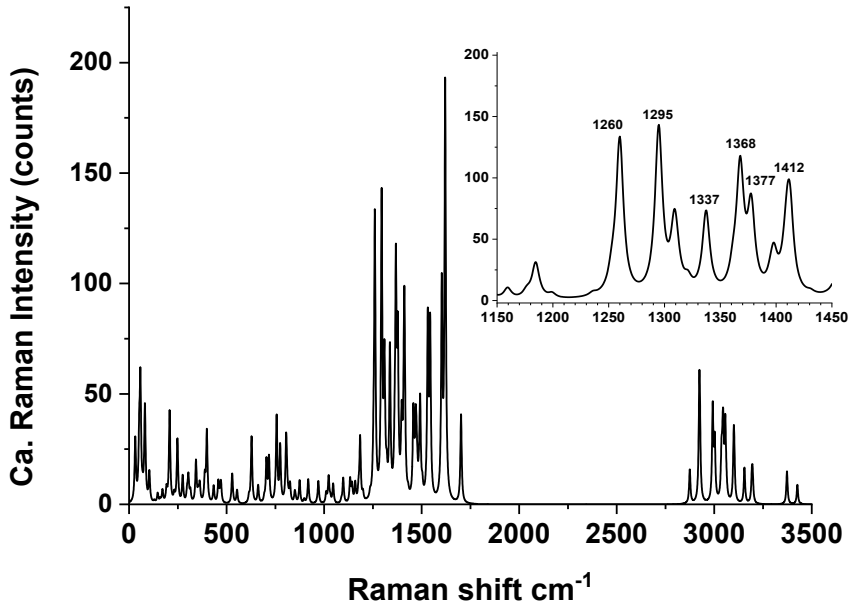

Figure S14: Calculated Raman spectrum for Nor$^+$. Inset shows a close-up of the 1150 – 1450 cm^{-1} region.

S.VII. 2D correlation of Nor^+ EC-SERS

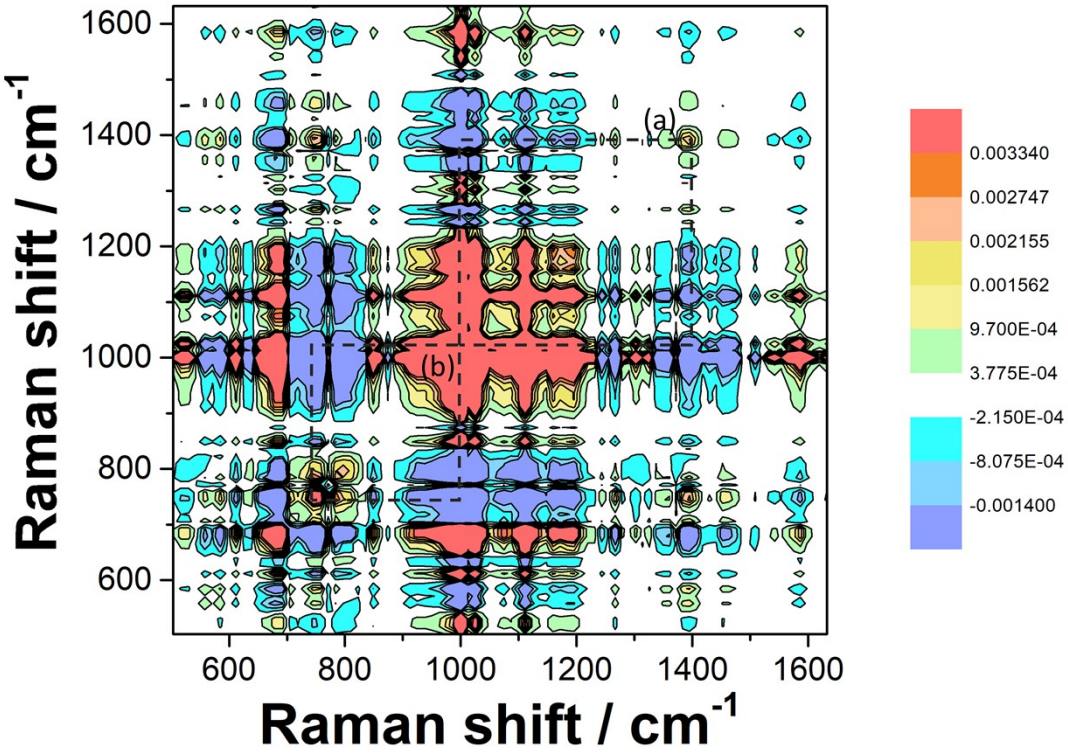

Figure S15: Synchronous 2D correlation for Nor+ (SERS data from Figure S9B). The correlation squares (a) & (b) symbolised the negative correlation between Nor^+ and BA^+ peak